Bowling Green State University

ScholarWorks@BGSU

Physics and Astronomy Faculty Publications

Physics and Astronomy

2007

Thermal properties of cubic KTa 1 x Nb x O 3 crystals

X. P. Wang

J. Y. Wang

H. J. Zhang

Y. G. Yu

J. Wu

See next page for additional authors

Follow this and additional works at: https://scholarworks.bgsu.edu/physics_astronomy_pub

Part of the Astrophysics and Astronomy Commons, and the Physics Commons

Repository Citation

Author(s)

X. P. Wang, J. Y. Wang, H. J. Zhang, Y. G. Yu, J. Wu, W. L. Gao, and Robert I. Boughton

X. P. Wang, J. Y. Wang, H. J. Zhang, Y. G. Yu, J. Wu, W. L. Gao, and R. I. Boughton

Articles you may be interested in

Cubic Sc 1 x Al x N solid solution thin films deposited by reactive magnetron sputter epitaxy onto ScN(111)
J. Appl. Phys. **105**, 113517 (2009); 10.1063/1.3132862

Growth and optical properties of KTa 1 x Nb x O 3 thin films grown by pulsed laser deposition on MgO substrates
J. Appl. Phys. **102**, 093106 (2007); 10.1063/1.2809400

Measurement of thermo-optic properties of Y 3 Al 5 O 12 , Lu 3 Al 5 O 12 , YAlO 3 , LiYF 4 , LiLuF 4 , BaY 2 F 8 , KGd (WO 4) 2 , and KY (WO 4) 2 laser crystals in the 80 – 300 K temperature range
J. Appl. Phys. **98**, 103514 (2005); 10.1063/1.2128696

Anisotropic thermal properties of monoclinic Yb : K Lu (W O 4) 2 crystals
Appl. Phys. Lett. **87**, 061104 (2005); 10.1063/1.2008360

Thermal and mechanical properties of BaWO 4 crystal
J. Appl. Phys. **98**, 013542 (2005); 10.1063/1.1957125

Thermal properties of cubic KTa$_{1-x}$Nb$_x$O$_3$ crystals

X. P. Wang,[1] J. Y. Wang,[1,a)] H. J. Zhang,[1] Y. G. Yu,[1] J. Wu,[1] W. L. Gao,[1] and
R. I. Boughton[2]
[1]*State Key Laboratory of Crystal Material, Shandong University, Jinan, Shandong 250100, China*
[2]*Department of Physics and Astronomy, Bowling Green State University, Bowling Green, Ohio 43403, USA*

Cubic potassium tantalite niobate [KTa$_{1-x}$Nb$_x$O$_3$ (KTN)] crystals of large size, good quality, and varying Nb concentration have been grown by the Czochralski method and their thermal properties have been systematically studied. The melting point, molar enthalpy of fusion, and molar entropy of fusion of the crystals were determined to be: 1536.9 K, 12 068.521 J mol^{-1}, and 7.85 J K^{-1} mol^{-1} for KTa$_{0.67}$Nb$_{0.33}$O$_3$; and 1520.61 K, 15 352.511 J mol^{-1}, and 10.098 J K^{-1} mol^{-1} for KTa$_{0.67}$Nb$_{0.33}$O$_3$, respectively. Based on the data, the Jackson factor was calculated to be 0.994f and 1.214f for KTa$_{0.67}$Nb$_{0.33}$O$_3$ and KTa$_{0.63}$Nb$_{0.37}$O$_3$, respectively. The thermal expansion coefficients over the temperature range of 298.15−773.15 K are: α=4.0268×10^{-6}/K, 6.4428×10^{-6}/K, 6.5853×10^{-6}/K for KTaO$_3$, KTa$_{0.67}$Nb$_{0.33}$O$_3$, and KTa$_{0.63}$Nb$_{0.37}$O$_3$, respectively. The density follows an almost linear decrease when the temperature increases=from 298.15 to 773.15 K. The measured specific heats at 303.15 K are: 0.375 J g^{-1} K^{-1} for KTaO$_3$; 0.421 J g^{-1} K^{-1} for KTa$_{0.67}$Nb$_{0.33}$O$_3$, and 0.430 J g^{-1} K^{-1} for KTa$_{0.63}$Nb$_{0.37}$O$_3$ The thermal diffusion coefficients of the crystals were measured over the temperature range from 303.15−563.15 K. The calculated thermal conductivity values of KTaO$_3$, KTa$_{0.67}$Nb$_{0.33}$O$_3$, and KTa$_{0.63}$Nb$_{0.37}$O$_3$ at 303.15 K are 8.551, 5.592, and 4.489 W m^{-1} K^{-1}, respectively. The variation of these thermal properties versus Nb concentration is qualitatively analyzed. These results show that crystalline KTN is a promising material for optical applications. © *2008 American Institute of Physics*. [DOI: 10.1063/1.2838221]

I. INTRODUCTION

In recent years, the development of large-capacity and highly functional metro or access networks has become a goal of researchers in information technology. In order to achieve this goal, the size and power consumption of optical devices must be reduced, while at the same time their functionality must be increased. Of these devices, optical modulators and optical switches are especially important for networks. The conventional materials typically applied in making these devices, such as LiNbO$_3$, have problems in terms of their large size and a relatively high driving voltage resulting from a small electro-optic effect. Attention has therefore been paid to the development of novel materials with a larger electro-optic effect with a view to overcoming these problems.[1]

Single crystal potassium tantalate niobate [KTa$_{1-x}$Nb$_x$O$_3$ (KTN)] is well known for its remarkable electro-optical, photorefractive, ferroelectric, and nonlinear-optical properties.[2–8] The most attractive property of KTN is its large quadratic electro-optic effect (Kerr effect), which determines device performance. The electro-optic coefficient of these KTN crystals is about 600 pm/V. This value is about 20 times larger than that of conventional LiNbO$_3$. In addition, the driving voltage of an optical switch fabricated with KTN is only 1/10th that of a conventional switch.[9] These results clearly show the excellent potential of KTN in terms of optical device performance. Single crystal KTN has, however, been considered impractical because it is difficult to grow.

By controlling the growth conditions such as temperature, thermal gradient, etc., precisely, we have grown large, good quality KTN crystals using the Czochralski technique.

Cubic KTN crystals, especially those near the cubic-tetragonal phase boundary, are reported to have the best known Kerr effect of any crystal material.[10] Interest in this kind of KTN is growing because a very large dielectric constant and Kerr coefficient can be obtained at room temperature. By using cubic KTN, excellent electro-optical elements and devices, which can be used at room temperature, can be designed and produced.[11]

Because a large, high quality KTN single crystal is very difficult to obtain, reports on the investigation of its properties are relatively rare. The thermal properties seriously affect the growth and application of a crystal. In the 1990s, Yang and Wang had investigated some thermal properties of KTa$_{0.63}$Nb$_{0.37}$O$_3$, which was grown by the flux pulling method. Their work was, however, concentrated in the temperature range of 130−370 K since their aim was to investigate the thermal effects in the phase transition process.[12–14] In this paper, we present measurements of the thermal properties, such as differential thermal analysis, thermogravimetric analysis (DTA/TA), specific heat, thermal conductivity, thermal expansion, etc., which have great influence on crystal growth and processing, and which greatly affect the possible application of KTN crystals. In order to qualitatively analyze the relation between thermal properties and Nb concentration, three KTa$_{1-x}$Nb$_x$O$_3$ crystals with different Nb concentrations (x=0, 0.33, and 0.37) were used in the experiments.

---

a)Author to whom correspondence should be addressed. Telephone: 86-531-88364340. FAX: 86-531-88564963. Electronic mail: jywang@icm.sdu.edu.cn.
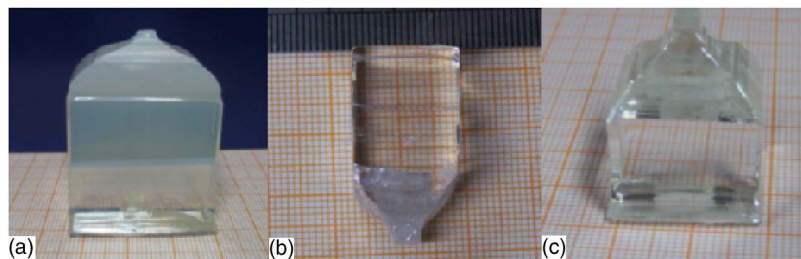
103, 033513-1

FIG. 1. (Color online) As-grown KTN crystals with different compositions and different size: (a) $KTaO_3$ 35 mm $\times$ 35 mm $\times$ 50 mm, (b) $KTa_{0.67}Nb_{0.33}O_3$ 15 mm $\times$ 15 mm $\times$ 20 mm, and (c) $KTa_{0.63}Nb_{0.37}O_3$ 20 mm $\times$ 20 mm $\times$ 15 mm.

II. EXPERIMENT

Polycrystalline $KTa_{1-x}Nb_xO_3$ was synthesized through a solid state reaction with the chemical reagents K_2CO_3, Ta_2O_5, and Nb_2O_5 (all of 99.99% purity) in a platinum crucible. KTN single crystals were grown in a TDL model-H50AC crystal pulling apparatus. The crucible was heated by using a 2 kHz intermediate frequency heater. The experiments were performed in an air atmosphere. The pulling rate was kept at 0.3–0.5 mm/h after the crystal diameter reached the target value. The crystal was rotated at a rate of 5–10 rpm during growth. After growth, the crystals were cooled to room temperature at a rate of 30−50 °C/h.[15] Because single crystal KTN is a solid solution of $KTaO_3$ (KT) and KNb_3O_3 (KN), it can be seen that it is difficult to grow a homogenous KTN crystal, from the phase diagram of KT–KN.[5] Changing the Nb/Ta ratio in the raw materials and temperature fluctuation during the crystal growth process can all cause variations in the (Nb/Ta) composition ratio of the crystal. In order to obtain a relatively homogenous crystal, some measures, such as using a big crucible which contains a sufficient mass of raw materials to grow the crystal, and growing the crystal at a relatively stable temperature, were adopted in our experiment. The detailed relationship between the Nb/Ta ratio in the raw materials, the growth temperature and Ta–Nb segregation were touched upon in our former work (Ref. 15). The compositions of the as-grown KTN crystals were measured by the electric probe microanalysis technique. Figure 1 shows the as-grown KTN crystals with Nb concentrations x =0, 0.33, and 0.37. The as-grown crystals exhibit no cleavage, no inclusions, no obvious striations, or other macroscopic defects. Also no light-scattering inclusions were observed when the crystals were illuminated under a 5 mW He–Ne laser. Clearly, the as-grown crystals possess good optical quality. X-ray powder diffraction shows that the as-grown KTN crystals belong to cubic phase at room temperature. The unit cell dimensions are a=0.3984, 0.3993, and 0.3996 nm for $KTaO_3$, $KTa_{0.67}Nb_{0.33}O_3$, and $KTa_{0.63}Nb_{0.37}O_3$, respectively.

A. Melting point and enthalpy of fusion measurements

The DTA method was used to determine the melting point and enthalpy of fusion for the KTN crystals of different composition. The measurement used a Perkin-Elmer diamond TA/DTA apparatus. Powder samples with weight up to 16.533 mg for $KTa_{0.67}Nb_{0.33}O_3$ and 11.007 mg for $KTa_{0.63}Nb_{0.37}O_3$ were used in the DTA measurement. The sample was kept in an Al_2O_3 crucible and another empty

Al_2O_3 crucible was used as reference while they were heated together at a constant rate of 10 K/min from 298.15 to 1603.15 K.

B. Thermal expansion measurement

The thermal expansion of the KTN crystals was measured over the temperature range from 298.15 to 773.15 K by using a thermal-mechanical analyzer made by Perkin-Elmer. The as-grown KTN crystal was cut into a rectangular shape with dimensions of $5.2 \times 5.5 \times 6.0$ mm$^3(a \times b \times c)$ for the thermal expansion measurement. The samples were oriented along its crystallographic a, b, and c axes. The samples were annealed at 1273.15 K for 15 h in order to release any processing stress. During the thermal-expansion measurements, the sample was heated at a constant rate of 5 K/min from 298.15 and 773.15 K and the thermal-expansion ratio versus temperature curves along the a, b, and c crystallographic directions were measured.

C. Density measurement

The density of the KTN crystals at room temperature was measured by the buoyancy method. The density can be calculated by

$$\rho = \frac{m_0\rho_{water}}{m - m'}, \tag{1}$$

where m_0 is the sample weight in air, m' is sample weight immersed in distilled water, and ρ_{water} is the density of distilled water at room temperature. With the samples used in the thermal expansion experiments, the density at room temperatures can be obtained.

D. Specific heat measurement

Specific heat was measured using a differential scanning calorimeter with a simultaneous thermal analyzer (NETZSCH model STA 449C). Double aluminum pans were used for the measurement in the following procedure: an empty sample pan together with another empty reference pan was heated first from 303.15 to 873.15 K at a rate of 10 K/min. Then the same operation was repeated with a KTN powder sample weighting 64.050 mg in the sample pan, and, finally, the results were obtained using the associated software.

E. The thermal diffusion coefficient measurement

The thermal diffusion coefficient of the $KTa_{0.67}Nb_{0.33}O_3$ and $KTa_{0.63}Nb_{0.37}O_3$ crystals was measured by the laser flash
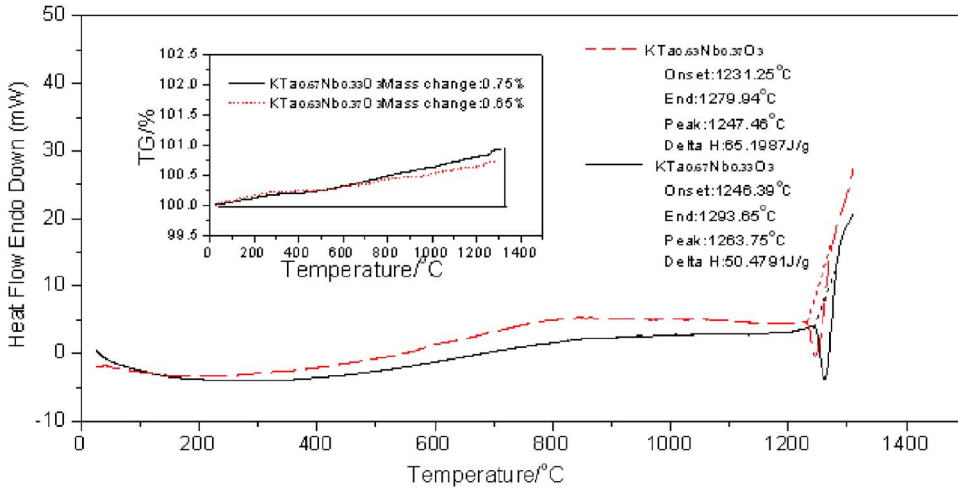
FIG. 2. (Color online) DTA and TA curves of KTN crystals.

III. RESULTS AND DISCUSSION

A. Melting point, enthalpy and entropy of fusion, and thermal gravimetric analysis

Since the melt growth of crystals takes place through the motion of the liquid-solid interface, $\Delta_{fus}H_m$ (the molar enthalpy of fusion) and $\Delta_{fus}S_m$ (the molar entropy of fusion) are important thermodynamic parameters, both for computer simulation and actual crystal-growth experiments. The roughness of the interface will determine the growth kinetics of the crystal.[16] Jackson showed that the roughness of the interface can be predicted by the Jackson factor,[17] which is given as

$$\alpha = \frac{L}{kT_E}f, \tag{2}$$

where L is the latent heat of crystallization, k is the Boltzmann constant, T_E is the melting point, and f is the fraction of the binding energy associated with the layer, which depends on the crystal face. If $\alpha \leq 2$, the interface is considered a rough surface; otherwise, it is considered a smooth surface.

Figure 2 shows the DTA and TA curves of the $KTa_{0.67}Nb_{0.33}O_3$ and $KTa_{0.63}Nb_{0.37}O_3$ crystals. From Fig. 2, a single sharp endothermic peak was observed in the temperature range between 1519.54 and 1566.8 K on the curve of $KTa_{0.67}Nb_{0.33}O_3$ and another single sharp endothermic peak was observed in the temperature range between 1504.4 and 1553.09 K on the curve of $KTa_{0.63}Nb_{0.37}O_3$. The peaks exhibit the characteristics of a first-order phase transition with peak temperatures at 1536.9 and 1520.61 K, respectively. We can identify these peaks as the melting points of the $KTa_{0.67}Nb_{0.33}O_3$ and $KTa_{0.63}Nb_{0.37}O_3$ crystals. Evidence of fusion of KTN crystals was found in the sample cell after the

DTA measurement. Compared with the melting points of $KTa_{0.67}Nb_{0.33}O_3$ and $KTa_{0.63}Nb_{0.37}O_3$, it can be concluded that the melting point decreases with an increase in Nb concentration in the KTN crystal. This result is in accord with the $KTaO_3 - KNbO_3$ phase diagram.[18] From the room temperature to the melting point, the DTA curves of two samples are almost invariant and exhibit no another peaks. This result indicates that the crystal has no first-order phase transition from room temperature to the liquid phase. In other words, $KTa_{0.67}Nb_{0.33}O_3$ and $KTa_{0.63}Nb_{0.37}O_3$ crystals maintain the cubic phase from room temperature up to the melting point. The TA curves also show that the total mass of the $KTa_{0.67}Nb_{0.33}O_3$ and $KTa_{0.63}Nb_{0.37}O_3$ crystals is nearly invariant over the measurement temperature range from 298.15 to 1583.15 K. This invariance has very important implications on the cooling process after the crystal growth process ends. A relatively high cooling rate can be chosen for a crystal that has no phase transition in the cooling process.

The molar enthalpy of fusion $\Delta_{fus}H_m$ of single crystal KTN was derived from the DTA curve using the area integration method included in the DTA analytical software provided by the Perkin-Elmer Co. The molar entropy of fusion $\Delta_{fus}S_m$ was calculated using the following thermodynamic equation:

$$\Delta_{fus}S_m = \frac{\Delta_{fus}H_m}{T_E}, \tag{3}$$

where T_E is the melting point of the crystal. The Jackson factor can be calculated by Eq. (4),

$$\alpha = \frac{L}{kT_E}f = \frac{\Delta_{fus}H_m}{RT_E}f = \frac{\Delta_{fus}S_m}{R}f. \tag{4}$$

The calculated results are listed in Table I.

It can be seen that the $\Delta_{fus}S_m/R$ of $KTa_{0.67}Nb_{0.33}O_3$ and $KTa_{0.63}Nb_{0.37}O_3$ is less than 2. That means the liquid-solid interface is most probably a rough surface when the crystal grows from the melt and explains why the crystal is difficult to grow. In our experiment, precise growth parameters were chosen to obtain high quality KTN crystals.

TABLE I. Thermodynamic parameters of KTN crystals obtained from DTA measurement.

Thermodynamic parameters	$KTa_{0.67}Nb_{0.33}O_3$	$KTa_{0.63}Nb_{0.37}O_3$
T_E (K)	1536.9	1520.31
$\Delta_{fus}H_m$ (J mol^{-1})	12 068.521	15 352.511
$\Delta_{fus}S_m$ (J K^{-1} mol^{-1})	7.85	10.098
α	0.944f	1.214f

B. Thermal expansion

The anharmonic vibration of the crystal lattice produces thermal expansion when the crystal is heated; the action of the anharmonic lattice vibrations is related to the structure and composition of the crystal and the force between the ions. The thermal expansion of a crystal has a great influence on crystal growth and on its possible applications.[19] The thermal expansion coefficient $[\alpha_{ij}]$ of a crystal is a symmetrical second-rank tensor.[20] In our experiment, the KTN crystals belongs to the cubic $m3m$ point group. In compliance with Neumann's principle, the thermal expansion of a cubic KTN should be isotropic and there is only one independent principal component of the thermal expansion coefficient tensor, which is $\alpha_{11}=\alpha_{22}=\alpha_{33}(\alpha_1=\alpha_2=\alpha_3)$. The values of α_1, α_2, and α_3 can be obtained by measuring the thermal expansion of a-, b-, and c-oriented crystal samples because $a//X_1$, $b//X_2$, and $c//X_3$.

The thermal expansion curves of KTN crystals with Nb concentrations $x=0$, 0.33, and 0.37 are shown in Fig. 3. It can be seen that the crystals exhibit only expansion when heated, which means that all the thermal expansion coefficients are positive. The average thermal expansion coefficient can be calculated by the following equation:

$$\bar{\alpha}_{(T0 \rightarrow T)} = \frac{\Delta L}{L_0} \frac{1}{\Delta T}. \tag{5}$$

Lines a, b, and c represent the expansion curves of $KTa_{0.63}Nb_{0.37}O_3$ along the principal axes. The measured mean linear coefficients of thermal expansion are $\alpha_a = 5.7495 \times 10^{-6}$/K, $\alpha_b = 5.3690 \times 10^{-6}$/K, and $\alpha_c = 6.5853$
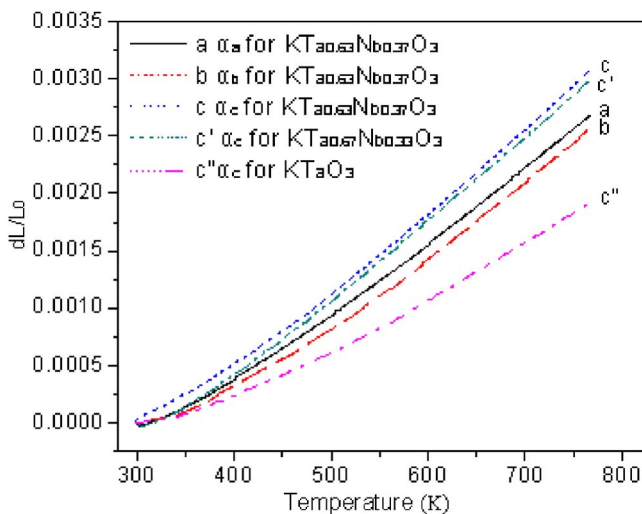

FIG. 3. (Color online) Thermal expansion curves of KTN crystals.

TABLE II. Theoretical and experimental density of cubic KTN crystals.

Crystal	$KTaO_3$	$KTa_{0.67}Nb_{0.33}O_3$	$KTa_{0.63}Nb_{0.37}O_3$
ρ_{theor} (g/cm^3)	7.035	6.231	6.181
ρ_{exper} (g/cm^3)	7.025	6.235	6.180

$\times 10^{-6}$/K, respectively. Considering the measurement error, we conclude that the (100) and (010) directions have similar expansion coefficients, whereas the expansion coefficient along the (001) direction is somewhat larger than those along the (100) and (010) directions. Two causes are responsible for this result. The first is the difference in homogeneity along these three directions. KTN is a crystalline solid solution. Changes in raw material concentration and growth temperature can all effect the Nb concentration in the KTN crystal.[18] In our experiment, the crystals were grown along the (001) direction. Fluctuation of the melt composition and the growth temperature can cause variation in the Nb concentration along different crystal growth directions, so the (001) direction is less homogeneous than in the other two directions, and therefore could lead to a bigger expansion effect in this direction.

Lines c' and c'' represent the expansion curve of $KTa_{0.67}Nb_{0.33}O_3$ and $KTaO_3$ along the (001) direction. The average linear coefficients are $\alpha_{c'} = 6.4428 \times 10^{-6}$/K and $\alpha_{c''} = 4.0268 \times 10^{-6}$/K, respectively. By comparing α_c, $\alpha_{c'}$, and $\alpha_{c''}$ we conclude that the thermal expansion coefficient of cubic KTN increases with increasing Nb concentration.

It should be noted that the difference between α_a, α_b, and α_c is quite small, in general agreement with the characteristics of a cubic crystal. Unlike anisotropic crystals, such as lithium niobate (LN) ($\alpha_{11}=14.1 \times 10^{-6}$/K and $\alpha_{33}=4.1 \times 10^{-6}$/K),[21] the approximately isotropic thermal expansion gives the KTN crystal many advantages. Whether during the cooling process after crystal growth, the machining process, or during beam irradiation, isotropic thermal expansion can reduce the inner stress caused by temperature fluctuations. Moreover, a relatively high cooling speed can be adopted after the crystal growth process is completed; the crystal is of higher quality and more useful for high power optical applications.

C. Density versus temperature curve of KTN crystal

The theoretical density value of cubic KTN at room temperature was calculated using

$$\rho_{theor} = \frac{MZ}{N_0 V} = \frac{M}{N_0 abc} = \frac{M}{N_0 a^3}, \tag{6}$$

where M is the molar mass of the crystal. The quantity Z represents the molecular number in one unit cell, which is unity for KTN. The quantity V is the volume of the unit cell and N_0 is the Avogadro constant. For cubic KTN, the theoretical density was calculated using Eq. (6) and the results are shown in Table II together with the experimental results. The results show that the calculated theoretical density is in good agreement with the experimental results on the crystals.
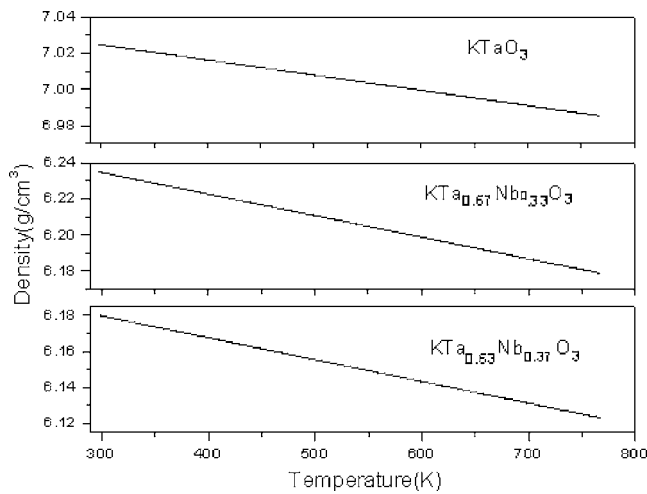
FIG. 4. Density vs temperature curves of KTN crystals.

FIG. 5. (Color online) Specific heat vs temperature curve of cubic phase KTN crystals.

Because of thermal expansion, the density of the crystals decreases with increasing temperature. Using the results obtained from the thermal expansion experiments and Eq. (7) (Ref. 22)

$$\rho = \frac{m}{abc} = \frac{m}{a^3} = \frac{m}{[a_0(1 + \Delta a/a_0)]^3} = \frac{\rho_0}{(1 + \Delta a/a_0)^3}, \quad (7)$$

where ρ_0 is the density of the crystal at T_0. The values of ρ_0 for KTaO$_3$, KTa$_{0.67}$Nb$_{0.33}$O$_3$, and KTa$_{0.63}$Nb$_{0.37}$O$_3$ were obtained by the buoyancy method and the results listed in Table II. The values of $\Delta a/a_0$ can be obtained from Fig. 3, where $T_0 = 298.15$ K.

The density versus temperature curves of KTaO$_3$, KTa$_{0.67}$Nb$_{0.33}$O$_3$, and KTa$_{0.63}$Nb$_{0.37}$O$_3$ over the temperature range from 298.15 to 773.15 K are shown in Fig. 4. It is noted that the densities decrease almost linearly with increasing temperature.

D. Specific heat analysis

The specific heat dependence of KTaO$_3$, KTa$_{0.67}$Nb$_{0.33}$O$_3$, and KTa$_{0.63}$Nb$_{0.37}$O$_3$ on temperature is shown in Fig. 5. It can be seen that the specific heat curves are almost constant with values of 0.371 -0.385 J g^{-1} K^{-1} (99.428$-$103.185 J mol^{-1} K^{-1}) for KTaO$_3$, 0.415$-$0.436 J g^{-1} K^{-1} (99.182 $-$104.201 J mol^{-1} K^{-1}) for KTa$_{0.67}$Nb$_{0.33}$O$_3$, and 0.421 -0.462 J g^{-1} K^{-1} (99.134$-$108.788 J mol^{-1} K^{-1}) for KTa$_{0.63}$Nb$_{0.37}$O$_3$, over the range from 303.15 to 843.15 K. This means that a change in temperature has little influence on the specific heat of the cubic KTN crystals. These results demonstrate that the specific heat value of KTN increases with increasing Nb concentration.

The specific heat of a substance can also be calculated according to the Dulong–Petit law when the temperature is above the Debye temperature θ_D.[23] According to the
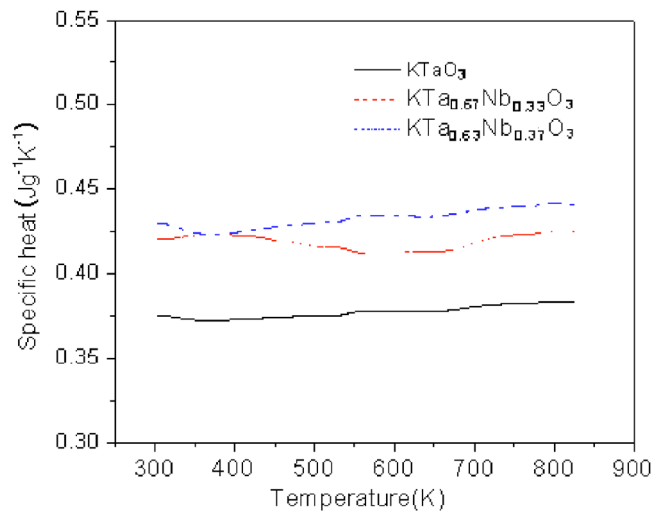
Dulong–Petit law, the specific heat of 1 mol atom is: $C_v \approx 3$ N K$=3$ R$=38.314$ J K^{-1} mol^{-1} ≈ 25 J K^{-1} mol^{-1}. But the specific heat of lighter elements, such as oxygen, is only 16.7 J K^{-1} mol^{-1}.[24] According to Kopp's law, the specific heat of 1 mol of a substance is the sum over all the atoms, so the specific heat of the KTN crystals can be calculated as follows:

$$C_v = 25 \times 1 + 25 \times 1 + 16.7 \times 3 = 100.1 \text{ J K}^{-1} \text{ mol}^{-1}.$$

Because there is little difference between C_p and C_v for a solid substance, we take the measured specific heat C_p to be equal to C_v, the specific heat at constant volume. It can be seen that the calculated value of C_v is in agreement with the measured value. These results show that the KTN crystal is in compliance with the Dulong–Petit law.

The specific heats of KTN crystals are 0.375 J g^{-1} K^{-1} for KTaO$_3$, 0.421 J g^{-1} K^{-1} for KTa$_{0.67}$Nb$_{0.33}$O$_3$, and 0.430 J g^{-1} K^{-1} for KTa$_{0.63}$Nb$_{0.37}$O$_3$ at 303.15 K, as shown in Table III together with those of LN.[21] The specific heat value of KTN is somewhat lower than that of LN. The lower specific heats of KTN would impose a larger internal gradient than LN when being irradiated by a laser beam.

E. Thermal diffusion coefficient and thermal conductivity

Knowledge of the thermal conductivity of a crystal is important from both fundamental and applied perspectives. The thermal conductivity $[k_{ij}]$ of a crystal is also a symmetrical second-rank tensor.[18] In the principal coordinate system, the $[k_{ij}]$ tensor is diagonal as is the thermal-expansion coefficient tensor and thus has only one independent principal component for a cubic crystal system. These components can be obtained by making measurements on a- (or b- or c-) oriented crystal samples.

TABLE III. Specific heat of KTN and LN crystals.

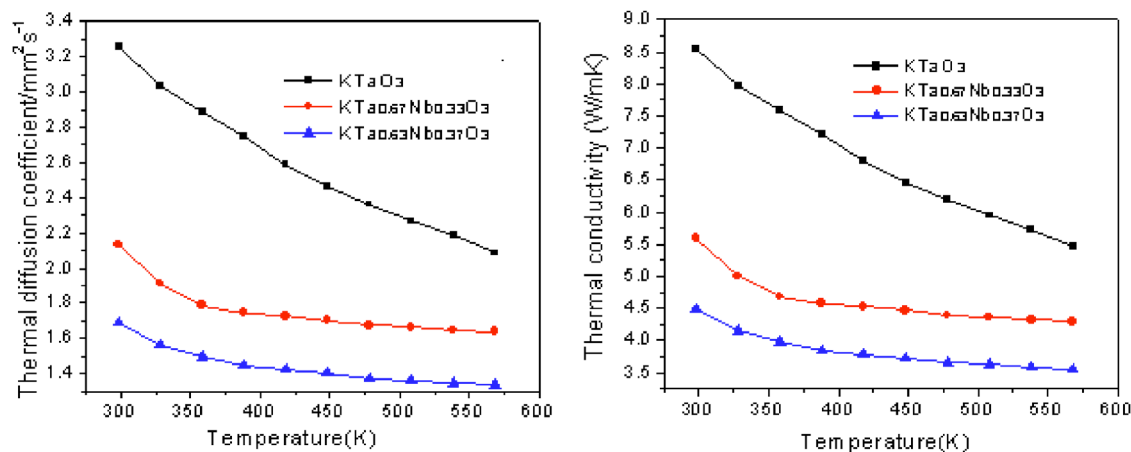| Crystal	KTaO$_3$	KTa$_{0.67}$Nb$_{0.33}$O$_3$	KTa$_{0.63}$Nb$_{0.37}$O$_3$	LN
Specific heat value (J g^{-1} K^{-1})	0.375	0.421	0.430	0.633

FIG. 6. (Color online) Thermal diffusion coefficient and the thermal conductivity curves of KTN crystals.

In our experiment, the thermal diffusion coefficient of the KTN crystals were measured directly and the thermal conductivity was calculated using

$$k = \lambda \rho C_p, \tag{8}$$

where k, λ, ρ, and C_p denote the principal thermal conductivity, the thermal diffusion coefficient, the density, and the specific heat of the crystal, respectively.

Figure 6 shows the thermal diffusion coefficient and thermal conductivity of $KTaO_3$, $KTa_{0.67}Nb_{0.33}O_3$, and $KTa_{0.63}Nb_{0.37}O_3$ over the temperature range from 303.15 to 573.15 K at 30 K intervals between measured temperature points. The thermal diffusion coefficient (left graph in Fig. 6) was measured by the laser flash method and the thermal-conductivity components (right graph in Fig. 6) were calculated according to Figs. 4 and 5 and the left graph in Fig. 6. From Fig. 6, it can be seen that the thermal diffusion and thermal-conductivity components decrease with increasing temperature. The thermal diffusion coefficient of $KTaO_3$ crystal is 3.259 mm^2 s^{-1} at 303.15 K, whereas the value for $KTa_{0.67}Nb_{0.33}O_3$ is 2.132 mm^2 s^{-1} and for $KTa_{0.63}Nb_{0.37}O_3$ is 1.689 mm^2 s^{-1} at that temperature. The calculated thermal conductivity values of $KTaO_3$, $KTa_{0.67}Nb_{0.33}O_3$, and $KTa_{0.63}Nb_{0.37}O_3$ at 303.15 K are 8.551, 5.592, and 4.489 W m^{-1} K^{-1}, respectively. We can therefore conclude that the thermal diffusion coefficient and thermal conductivity decrease with increasing Nb concentration.

IV. CONCLUSION

The thermal properties of cubic KTN crystals were carefully studied by measuring the melting point, molar enthalpy of fusion, molar entropy of fusion, thermal expansion, specific heat, and thermal diffusion coefficient. The variation of these thermal properties versus Nb concentration (x value) is qualitatively analyzed. The DTA/TA measurement shows that the crystal possesses relatively small molar entropy of fusion and that the melting point decreases with increasing x. The thermal-expansion measurements show that the thermal-expansion coefficient tensor of single crystal KTN has only one independent principal component and its value increases with increasing x. The specific heat of the crystal is little changed over the temperature range from 303.15 to 843.15 K

and its value increases with increasing x. The high value of the thermal conductivity tensor components suggests that the crystal has good thermal conduction properties. In conclusion, the thermal properties of cubic KTN indicate that the crystal is a promising material for optical applications.

[1]III-Vs Review **16**, 25 (2003).
[2]R. Pattnaik and J. Toulouse, Phys. Rev. Lett. **79**, 4677 (1997).
[3]L. A. Knauss, K. S. Harshavardhan, H. M. Christen, H. Y. Zhang, X. H. He, Y. H. Shih, K. S. Grabowski, and D. L. Knies, Appl. Phys. Lett. **73**, 3806 (1998).
[4]P. B. Ishai, C. E. M. de Oliveira, Y. Ryabov, Y. Feldman, and A. J. Agranat, Phys. Rev. B **70**, 132104 (2004).
[5]J. Y. Wang, Q. C. Guan, J. Q. Wei, and Y. G. Liu, J. Cryst. Growth **116**, 27 (1992).
[6]Q. C. Guan and J. Y. Wang, Appl. Phys. Lett. **16**, 63 (1993).
[7]F. S. Chen, J. E. Geosic, S. K. Kurtz, J. G. Skinner, and S. H. Wenple, J. Appl. Phys. **1**, 37 (1966).
[8]R. Hofmeister, A. Yariv, and S. Yagi, Phys. Rev. Lett. **9**, 69 (1992).
[9]R&D Information, NTT Tech. Rev. **1**, 56 (2003).
[10]Y. M. Abdulraheem, A. L. Gentile, and O. M. Stafsudd, J. Appl. Phys. **100**, 104111 (2006).
[11]M. DiDomenico, Jr. and S. H. Wemple, Phys. Rev. **166**, 565 (1968).
[12]M. Wang, J. Y. Wang, Y. G. Liu, Q. C. Guan, and J. Q. Wei, Ferroelectrics **49**, 132 (1992).
[13]M. Wang, Z. H. Yang, J. Y. Wang, Y. G. Liu, Q. C. Guan, and J. Q. Wei, Ferroelectrics **55**, 132 (1992).
[14]Z. H. Yang, Q. C. Guan, J. Q. Wei, and J. Y. Wang, J. Therm. Anal. **297**, 45 (1995).
[15]X. P. Wang, J. Y. Wang, Y. G. Yu, H. J. Zhang, and R. I. Boughton, J. Cryst. Growth **398**, 293 (2006).
[16]D. Elwell and H. J. Scheel, *Crystal Growth from High-Temperature Solutions* (Academic, London, 1975), p. 138.
[17]K. A. Jackson, *Liquid Metals and Solidification* (ASM, Cleveland, 1958), p. 174.
[18]H. J. Scheel, J. Cryst. Growth **12**, 211 (2000).
[19]W. B. Hou, D. Xu, D. R. Yuan, M. G. Liu, N. Zhang, X. T. Tao, S. Y. Sun, and M. H. Jiang, Cryst. Res. Technol. **939**, 29 (1994).
[20]F. Nye, *Physical Properties of Crystals* (Oxford University Press, Oxford, 1985).
[21]D. Taylor, EMIS Data Reviews Series No. 5, 1989.
[22]W. Ge, H. Zhang, J. Wang, J. Liu, X. Xu, X. Hu, and M. Jiang, J. Appl. Phys. **98**, 013542 (2005).
[23]M. Born and K. Huang, *Dynamical Theory of Crystal Lattices* (Oxford University Press, Oxford, 1954), p. 38.
[24]Z. D. Guan, Z. T. Zhang, and J. S. Jiao, *Physical Properties of Inorganic Materials* (Tsinghua University Press, Beijing, China, 1992).